Modelling the kinetic of ethylene reaction with metallocene catalysts

Ana C. Oliveira[a], M. Rosário Ribeiro[a], Timothy F. McKenna[b]

[a] Chemical Engineering Department, Instituto Superior Técnico, Lisbon, Portugal
[b] CNRS-C2P2 /ESCPE-Lyon, BP 2077, 43 Blvd du 11 Novembre 1918, 69616 Villeurbanne, France

Abstract

The purpose of this work was to study and model the kinetics of two different metallocene catalysts supported on silica pre-treated at different dehydroxylation temperatures that are $(EtInd)_2ZrCl_2$ and $(n\text{-}BuCp)_2ZrCl_2$. Results have shown that single site model comprising non-instantaneous activation and 1st order decay exhibits the best fitting to experimental kinetic data.

Then, to understand how the microstructure of the polyethylene produced, is affected by silica dehydroxylation temperature and reaction time, GPC analysis was used to determine the MW distribution of polymer chains.

It was possible to correlate MWD with a multiplicity of active sites with deconvolution model. In order to characterize the multiple nature of those active sites during polymerization, MWD were deconvoluted based on Flory distributions. This topic was studied just for the catalyst that gives broader MWD. Results point out the presence of 2 to 3 different active sites families that may change with time. This kind of studies with help of models can significantly improve our understanding of the catalyst behavior and provides additional tools for catalyst and process control.

Keyword **- Supported Metallocene, Modelling Kinetic, Dehydroxylation Temperature, Polymer Microstructure.**

1. INTRODUCTION

Polyolefins are the largest group of thermoplastics, often referred to as commodity thermoplastics. The two most important and common polyolefins are polyethylene and polypropylene and they are very popular due to their low cost and wide range of applications.

At the heart of all polyolefin manufacturing processes is the system used to promote polymer chain growth. For industrial applications, polyethylene is made with either free radical initiators or coordination catalysts. Coordination catalysts, especially metalocene catalysts, can control polymer microstructure much more efficiently than free radical initiators and are used to make polyolefins with a wide range of properties.

Ethylene polymerization processes can operate with homogeneous catalysts in solution reactors or with heterogeneous catalysts in two-phase or three-phase reactors. Usually, olefin polymerization is carried out by using catalyst supported on porous supports. These catalysts are preferred in industry because they lead to well define polymer morphology and reduce drastically reactor fouling. The support also helps to maintain the particle integrity controlling better the microstructure.

Between all types of catalyst, heterogeneous metallocenes supported on MAO/ silica will be used in this work. By making a thermal treatment to Silica, the surface composition may be changed by controlling the type and proportion of the different groups, silanol and silxane. During the heating water is removed in a first place (dehydration) then the hydroxil groups react forming siloxane groups that are desirable to react with catalyst. The temperature used in dehydroxylation procedure affects deeply the catalyst performance on reaction.

The main scope of this thesis is to understand how this temperature effect polymerization kinetics and to determine the main kinetic parameters of reaction. This way, different approximations, namely instantaneous or non-instantaneous site activation and first or second order deactivation, will be applied to a general model for the kinetics of single site catalysts general single site. The fitting of the experimental data to the alternative models will allow to determine which model describes better the systems under study.

Supported catalyst present some heterogeneity resulting in multiple-site-type catalytic systems that typically exhibit broad molecular weight distribution (MWD). This behavior can be estimated by polydispersity index (DPI) which measures the heterogeneity of polymer chain sizes, given by the ratio between Mw and Mn.

Deconvolution of MWD is a new approach to identify the number of active site types and chain microstructures produced on each active site type.

1.1 Metallocene catalysts

Metallocenes are composed of a transition metal atom sandwiched between two rings and two atoms of Chloride. The rings, also called ligands, can be connected through a bridge B in figure 1, which is responsible to vary the angle between the rings. In general they have the formula $Ring_2BMCl_2$, where B is the bridge between both rings, M is the metal and R represents other groups linked to the rings.

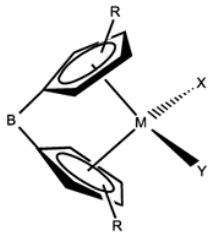

Figure 1 - basic structure scheme of metallocene

It´s possible to change the ligand type, type of bridge and type of transition metal atom. A large variety of metallocene catalysts can be obtain by altering the simple structure of a zirconium base catalyst.

1.2 Supported catalysts

Despite the high polymerization activities, homogeneous metallocenes suffer some drawbacks like the lack of control of polymer morphology and reactor fouling. Therefore for the practical applications the immobilization of metallocene compounds on a support is required. The key point is finding a way to anchor the metallocene onto the support without losing the advantages of homogeneous complex like high activity, stereochemical control and improved morphology required for industrial applications. The nature of support as well as the technique plays an important role in catalytic activity and polymer properties such as MWD.

The most commonly used support for single-centre catalysts are silica particles. Silica exists in a number of crystalline phases but for catalyst support amorphous silica is normally used. This is by far the most common support used in the heterogenization of single-centre olefin polymerization catalysts, as it has high surface area and porosity, good mechanical properties and is stable and inert under reaction and processing conditions. The properties of amorphous silica are mainly governed by the surface chemistry and specially by the presence and distribution of silanol groups. Three different types of silanol groups can be distinguished (a) geminal, (b) vicinal and (c) isolated

Before the anchoring process, silica requires a thermal treatment to remove water and reduce the hydrogen bridges between silanol groups on the surface and leading to siloxane bridges. Hydrogen bonded water molecules need temperatures up to 180ºC. Up to this temperature the adjacent vicinal silanol groups condense with each other to form siloxane bridge which are desirable to react with MAO.

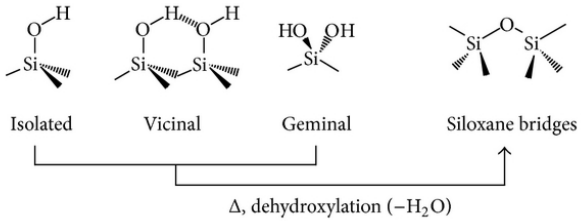

Figure 2 - partial dehydroxylation of the silica surface

The dehydroxylation temperature of the thermal treatment is usually chosen in order to remove residual water and hydroxyl groups, but it also depends on several factors such as the polymerization process, the supporting technique, and the cocatalyst and (pre)catalyst combination. The dehydroxylation temperature affects deeply the ability of the support to anchor the different species.

After silica thermal treatment the cocatalyst (normally an aluminoxane) and (pre)catalyst are impregnated in the support.

There are three basic methods of supporting aluminoxane-activated single-site catalyst:

1. Supporting the aluminoxane and then reacting with (pre)catalyst
2. Supporting the (pre)catalyst and then reacting with aluminoxane
3. Contacting the aluminoxane and (pre)catalyst in solution before supporting

Method 2 consists in adsorbing the metallocene on the support and then reacting it with cocatalyst. In this method, the silanol isolated groups of silica, bond to chlorine of catalyst by via μ-oxo bonding. But if it still remains vicinal and germinal groups, when contacts with catalyst, there are a consume of the two chlorines in immobilization catalyst process as in (b) of fig 3, and as a result we have less active sites because the inadequate linkage between the support and metallocene.

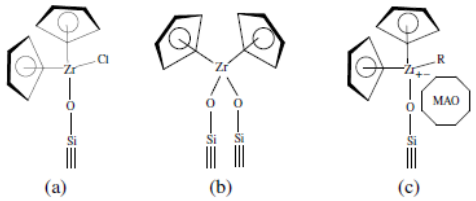

Figure 3 – Direct immobilization of metallocene on isolated (a) and vicinal (b) silanol groups of silica. Catalyst activated before MAO impregnation (c)

To prevent deactivation of these supported systems by reaction with silanol functionalities, it is common to use the first method, that chemically anchors the silica surface with an aluminoxane, in the present case, methyaluminoxane, known as MAO.

Supporting MAO first, followed by reaction with a metal complex, is the most frequently used and commercially available methods used to prepare heterogeneous single-center polymerization catalysts.

In method 3, the metallocene and the cocatalyst are precontacted before supporting

4. EXPERIMENTAL

2.1 Material

Silica (Grace 948) was used as a support catalyst. The diluent used for slurry was heptane with add of 1ml of TiBA to clean the impurities. The two types of catalyst study were: Ethylenebis(Indenyl) Zirconium Dichloride - $(EtInd)_2ZrCl_2$ and Butylcyclopentadienyl Zirconium Dichloride - (n-BuCp)2ZrCl2. MAO was the cocatalyst.

2.2 Preparation of supported catalyst

Silica is introduced in a Schlenck tube and placed under vacuum and then is dehydroxynated using the temperature program of figure 4.

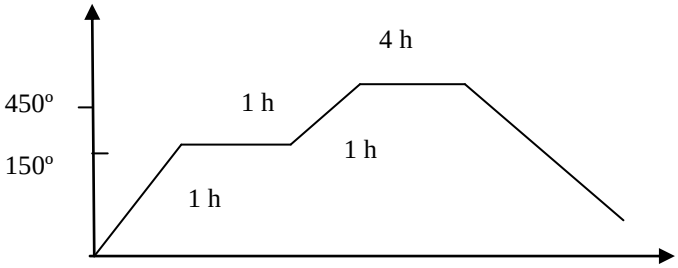

Fig. 4 - Dehydroxylation Temperature program for 450ºC

The silica dehydroxylation temperatures used for each catalyst are in table I.

For Impregnation of SMAO (silica+ MAO), 2 g of silica dehydroxilated was introduced with a solution of MAO in toluene (30%) in a flask equipped with mechanical agitation under argon. And remained during 4 hours at 80ºC. The suspension was then washed with toluene and the residual solid is dried under vacuum.

SMAO is then reacted with the catalyst in hot toluene in a flask equipped also with agitation and under argon. The amounts of MAO and metallocene were calculated in the way to have an Al/Zr molar ratio of 150. The mixture is stirred at 50ºC during 1 hour. After the reaction the solid is again washed with toluene and then dried under vacuum.

Second serie of catalyst			
$(n\text{-}BuCp)_2ZrCl_2$	**200ºC**	**450ºC**	**600ºC**

TABLE I
DEHYDROXYDATION TEMPERATURES

First serie of catalyst		
$Et(Ind)_2ZrCl_2$	**450º C**	**600ºC**

2.2 Slurry phase polymerization in semibatch reactor (with continuous feed of ethylene)

The reactor used in this experiment is a 2,5 L reactor in steel with an spherical shape called turboshefere. It´s equipped with a three blade stirrer and a four mouths, one for the argon and monomer entry, one used for the vacuum and also exhausted air, and another for the entry of the mixture. The temperature is controlled by a jacket around the reactor with water circulating either for cooling, either for heating (with water from a warm bath). The stirring have also a refrigiration cooling system with water circulating.

Before start a reaction, the reactor needs to be heat up to 80ºC and filled with argon and then vacuum three times during at least 1 hour. These cycles are made in order to clean the impurities inside the reactor. The same precedure was made in the 2-neck Schlenk that contain the reactional mixture. After cycles proceed, this 2-neck Schlenk is filled with 500ml of heptene (diluent) and 1 ml of solution TiBA in heptane (1M). In the glove box is placed an amout of catalyst (preferably the same amount each batch) in a small two-neck Schlenk. Experiments were than in the glove only when concentrations of oxygen were below 20 ppm.

After that, the mixture is injected into the reactor meanwhile cooled and the stirring speed adjusted around 350 rpm.

At last, the reactor is heated again to 80ºC and after reach this temperature, the monomer valve is open to handle a total pressure of 9 bar (8 bar of ethylene + 1 bar of argon), to start the polymerization.

The starting point of the reaction is when ethylene started to be consumed and we see a decrease in ethylene presure in the ballast. After that it is taken mesures of the pressure inside the ballast (controled by a pressumeter spy) minute by minute.

Once the reaction is finished the monomer inlet is closed and the reactor is rapidly cooled down and depressurized with exahusted outlet mouth. To recover the polymer, the reactor is open with an hydraulic sytem and then cleaned with heptane. To get the powder, the heptane-polymer is filtrated into a vacuum filter and then dryed in a vacuum chamber to remove the remains of diluent.

5. MODEL DEVELOPMENT

A complete process of modelling is very complex and involves not only the microscale, but also the mesoscale and macroscale. Macroscale(>1 m) takes into account the modelling of hydrodynamics inside the reactor.

In mesoscale ($> 10^{-3} – 10^{-2}$ m) is modelled the temperatures and monomer concentration gradients in interparticle,intraparticle and particle-wall. At this scale these gradients of depends on the size, porosity and structure of the catalyst and the concentration of polymer created inside the particle, which interfere with the growing of polymer chain. At microscale, is modelled the phenomenas that occur at the catalytic active sites, like diffusion of monomer in microspores and polymerization kinetics. This phenomenas effect the microstructure formation of MWD and are responsible for long and short chain branches. In the present case, only microscale will be considered, this means that after achieving the stationary state, the kinetic is the limiting step regarding to mass transfer resistances.[3]

The strategy for creating a mathematical model that describes the behavior of homopolymerization kinetics is to find out first all the possible reactions that occur in the reactor mixture and then develop a population balance equation for each component.

The main steps in coordination polymerization mechanism include activation, propagation, transfer and deactivation between the components of the mixture. Some of the mechanisms that could occur in reaction are described in table II.

General Model of kinetics single site

TABLE II
REACTION MECHANISMS

Mechanism	
Activation step	$C \xrightarrow{ka} P_0$
Propagation step	$P_n + M \xrightarrow{kp} P_{n+1}$
Chain transfers to monomer	$P_n + M \xrightarrow{ktm} P_1 + D_r$
Catalyst deactivation	$C_* \xrightarrow{kd*} D_*$
Catalyst Impurity deactivation	$C_* + I \xrightarrow{kdi*} D_*$
Polymer Impurity deactivation	$P_n + I \xrightarrow{kdi} P_n + D_*$

C - catalyst M - monomer P_n - polymer chain with n monomers C* - catalyst active D* - catalyst deactivated I - impurity ka – activation kinetic canstant kp - propagation kinetic canstant kd* - deactivation kinetic constant kdi/kdi* - deactivation with impurities kinetic constant ktm – monomer transfer kinetic constant

In single site models, only activation, propagation, and polymer deactivation are considered.

The polymerization rate, Rp is given by the equation 1.1.

$$R_p = -\frac{d[M]}{dt} = k_p[M_s][Y_0] \qquad (1.1)$$

In this case we have a semibatch reactor, so the polymerization rate can be equal to the monomer feed divided by the volume of the reactor.

$$R_p = \frac{F}{V_r} \qquad (1.2)$$

The balance of active sites in the reactor is given by equation 1.3

$$\frac{d[C^*]}{dt} = -k_a[C^*] \quad (=) \quad [C^*] = [C_0]e^{-k_a t} \qquad (1.3)$$

The initial concentration of active sites in the reactor for heterogeneous catalysts is given by the molar fraction of catalyst.

$$[C_0] = \frac{x_c\, W_c}{M_{m_c}} \qquad (1.4)$$

Knowing that 1 mole of Zr is equivalent to 1 mole of catalyst $(n\text{-buCp})_2ZrCl_2$ or $(EtInd)_2Cl_2$) we can calculate the

fraction of catalyst moles knowing the Zr (wf) content (g/100g of total supported catalyst) obtain by elemental analysis.

$$x_c = \frac{Zr\ (wf)\ \times M_m\ (cat)}{M_m(Zr)} \qquad (1.5)$$

Despite having a mass of catalyst with a molar number of active sites determined by elementary analysis, only a small fraction of active centers is active. This value is around 10% (ε) [2]

$$\left[\widetilde{C_0}\right]_{(t=0)} = \varepsilon \times [C_0] \qquad (1.6)$$

For calculating the Concentration of monomer in the polymer, once we are considering the concentration of monomer in the polymer and it´s a slurry semibatch reactor, we have a gas-liquid and solid phase, so it needs to be considered the gas-liquid and liquid-solid monomer concentration. To simplify the problem some assumptions are taking into account.

- The concentrations in both phases are in equilibrium. Since the reactor is semibatch with continuous ethylene feed to keep the pressure constant, there is no variation of concentration of monomer if the equilibrium is achieved.
- It was assumed a linear relationship between concentrations in two phases using partition coefficient in respect/in terms of monomer partial pressure.

$$[M]_g = z\frac{P_M}{RT} \qquad (1.6)$$

$$[M]_l = K_{g-l}\, z\frac{P_M}{RT} = K^*_{g-l} P_M \qquad (1.7)$$

$$[M]_s = K_{l-s}\,[M]_l = K_{l-s}K^*_{g-l}P_M = K'_{g-s}P_M \qquad (1.8)$$

Since we don´t know K´g-s, will be calculate an apparent kinetic rate constant, k^*_p.

The general rate equation will became as in equation 1.9

$$R_p = k_p K'_{g-s} P_M = k^*_p P_M \qquad (1.9)$$

3.1 Instantaneous activation single site models

Given the general model presented before several approximations may be considered such as: instantaneous or not instantaneous site activation and first or second order deactivation.

In this section the dependence of Rp with time for instantaneous activation and first order deactivation will be developed

3.1.1 Model First order deactivation

In instantaneous mode, catalyst activation ka, which is the constant activation of catalyst for reaction, is zero due to the fast reaction start.

$$\frac{d[Y_0]}{dt} = \overbrace{k_a[C^*]}^{=0} - k_d[Y_0] \qquad (2.0)$$

solving equation 2.0 simultaneous with equation 1.1 and 2.6 for initial condition of $[Y_0](t=0)=[C_0]$, we obtain the following solution.

$$\mathrm{Rp} = k_p{}^* P_M \times \varepsilon[C_0]\mathrm{e}^{-\mathrm{kdt}} \qquad (2.1)$$

For the first order decay kinetics and instantaneous site activation, the logarithm of polymerization has to be a linear function of time. So if experimental data does not show a linear correlation between Rp and time, it means that this is not the operating mechanism for the tested conditions.

$$Ln\ R_p = Ln\left(k^*{}_p P_M \varepsilon[C_0]\right) - k_d t \qquad (2.2)$$

3.1.2 Model Second order deactivation

The only difference between this model and the previous is that the deactivation result from a bimolecular deactivation mechanism. And so equation 2.0 turns into equation 2.3, with exponent 2.

$$\frac{d[Y_0]}{dt} = -k_d{}^*[Y_0]^2 \qquad (2.3)$$

Solving the previous equation we obtain equation 2.4.

$$[Y_0] = \frac{\varepsilon[C_0]}{1 + \varepsilon[C_0]k_d{}^* t} \qquad (2.4)$$

This equation is solved simultaneous with equation 1.1 for the same initial condition. Following the same development done for 1th order deactivation model we can obtain a linear relation between 1/Rp and time.

$$\frac{1}{Rp} = \frac{1}{k_p{}^* P_M \varepsilon[C_0]} + \frac{k_d{}^*}{k_p{}^* P_M} t \qquad (2.5)$$

3.2 Non-instantaneous activation single site models

For first order deactivation without instantaneous activation, the system of equations to solve is the following.

$$\frac{d[C]}{dt} = -k_a[C^*] \quad (=) \quad [C^*] = [C_0]e^{-k_a t} \qquad (2.6)$$

$$\frac{d[M_s]}{dt} = -k_p{}^* P_M \qquad (2.7)$$

$$\frac{d[Y_0]}{dt} = (k_a)[C^*] - kd[Y_0] \qquad (2.7)$$

3.2.1 Second order deactivation

For second order deactivation model the set of equation to be solved comprise the previous set of equations, where equation 2.7 was replaced by equation 2.8.

$$\frac{d[Y_0]}{dt} = (k_a)[C^*] - kd^*[Y_0]^2 \qquad (2.8)$$

To solve these differential equations the numerical solution Runge-Kutta 4 order was used.

In the following sections these models will be used to fit the experimental kinetic data obtained for the catalytic systems studied, in order to determine which type of activation and deactivation model operates.

6. DECONVOLUTION APROACH

Since the catalyst is supported, several types of active sites with a different accessibility and reactivity are present, giving rise to polymer chains with different properties namely MWD. The MWD obtained in SEC analysis reflects the contribution of each type of active sites on the overall polymer microstructure. This way, it´s assumed that the overall MWD will be the sum of MWD of each type of active site. In order to determine the number of active site types, their contribution and how they evolve along reaction, deconvolution model was used.

In this model chain formed on each active site type assumed to follow Flory´s distribution with PDI a fixed of 2 corresponding to single site typical PDI. The parameters are estimated with minimizing the sum of the squares of differences between experimental (SEC) and model data.

The MWD model deconvolution used is described in appendix 3.

With this model we could impose the number of families and compare which one fits better the experimental data. For each family assumed, we obtain a MWD curve with a specific Mw and Mn.

he model was simulated in an excel file provided by Prof. r. João B. P. Soares and Prof. Dr. Timothy F. L. Mckenna. [2]

7. RESULTS AND DISCUSSION

5.1 Instantaneous modelling results

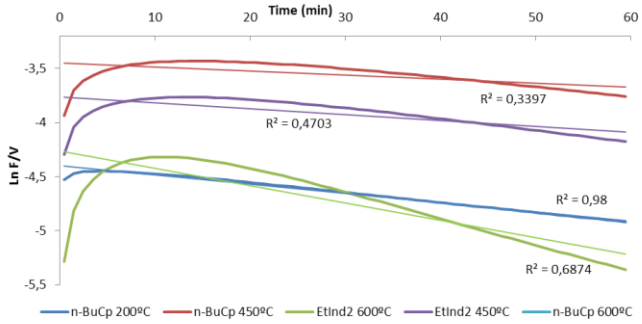

Fig. 5 Results of experimental data linearized and respective correlation line given by instantaneous activation 1st order decay model

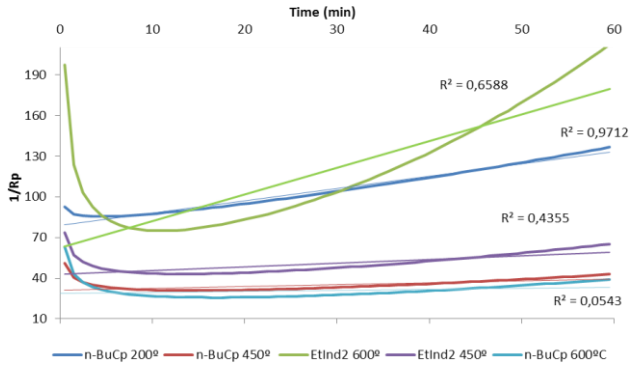

Fig. 6 Results of experimental data linearized and respective correlation line giving by noninstantaneous 1º order decay model

The experimental data obtained for the different catalysts studied was fitted to these linear equations. Figures 5 and 6 show respectively the experimental values of Ln Rp and 1/Rp versus time and the derived equations from linear regression, obtained in excel. As it may be seen from these plots and from the rather low values for R^2 these models do not fit well to the experimental data. This means that activation step is not instantaneous for none of the catalysts.

However, it´s possible to see that the one which is more close to linearity is n-BuCp 200ºC, with R-Square of 0,98 for instantaneous1º order decay and R-Square of 0,9712 for instantaneous 2º order decay.

In this case the Rp profiles were not plotted since from the previous fitting we concluded instantaneous model is not appropriate to explain the kinetics of this polymerization reaction

5.2 Non-instantaneous modelling results

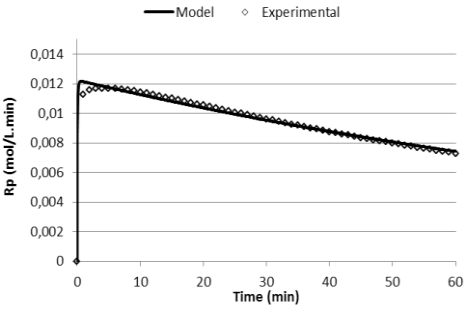

Fig. 7 Run 1

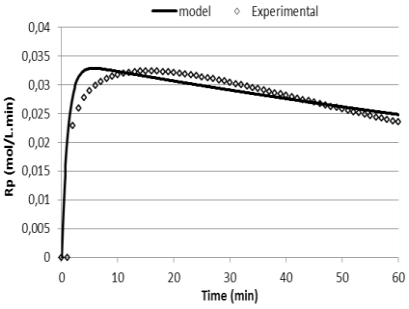

Fig. 9 Run 3

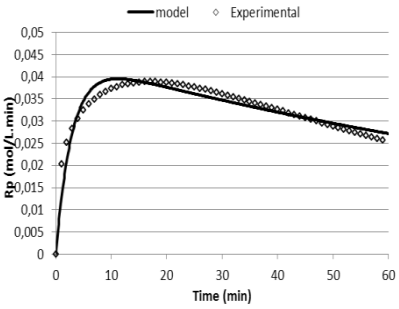

Fig. 11 Run 5

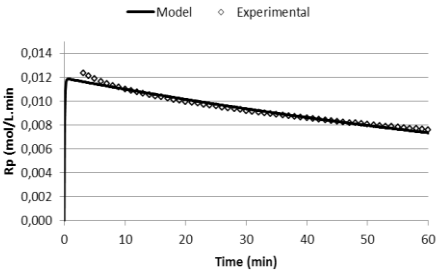

Fig. 8 Run 2

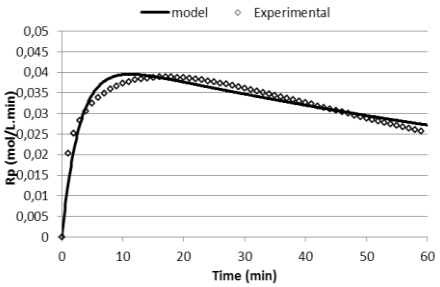

Fig. 10 Run 4

TABLE III – KINETIC PARAMETERS FOR $(n\text{-BuCp})_2ZrCl_2$ 200ºC, 450ºC AND 600ºC

Run	Catalyst type	Catalyst Mass (mg)	Pm (bar)	[C0] (mol/L)	ka (min^{-1})	kp* ($L.mol^{-1} bar^{-1}min^{-1}$)	kd (min^{-1})
1	n-BuCp 200ºC	26	8,2	$6,27 \times 10^{-7}$	12,3	$2,22 \times 10^{4}$	$8,34 \times 10^{-3}$
2	n-BuCp 200ºC	24	8,5	$5,79 \times 10^{-7}$	12,3	$2,26 \times 10^{4}$	$9,69 \times 10^{-3}$
3	n-BuCp 450ºC	25	8,0	$1,64 \times 10^{-6}$	$9,15 \times 10^{-1}$	$2,44 \times 10^{4}$	$5,27 \times 10^{-3}$
4	n-BuCp 450ºC	28	8,1	$2,82 \times 10^{-6}$	$7,64 \times 10^{-1}$	$1,68 \times 10^{4}$	$5,25 \times 10^{-3}$
5	n-BuCp 600ºC	26,5	8	$2,72 \times 10^{-6}$	$3,44 \times 10^{-1}$	$1,98 \times 10^{4}$	$8,15 \times 10^{-3}$

When comparing the kinetic parameters obtained from experiments performed in the same conditions it is possible to notice that the values of ka, kd and kp* are similar having the same order of magnitude.

In what concerns ka values, it is possible to see that n-BuCp 200ºC presents the higher ka value of 12.3 min-1. This is in accordance to the fact that the maximum of activity was attained in 1 minute of reaction The smaller activation constant, ka=0,344 min^{-1} was obtained for 600ºC. In this case it takes 11 minutes of reaction to attain the maximum of activity, For 450ºC the maximum activity was observed for 6 minutes and ka value is around 0,8 min^{-1}.(average of two experiments)

Regarding de deactivation, given by kd value, the higher value was for n-BuCp 200ºC and the lower one for n-BuCp 600ºC. Meaning that silica dehydroxydation at 600ºC followed by subsequent gives more stability in terms of activity than 200ºC in n-BuCp case.

Concerning kp apparent value, we can observed that the values are close with just a few deviation, with values around $2,2x10^4$ $L.mol^{-1}bar^{-1}$, which means that in all experiments were used similar conditions of pressure and temperature.

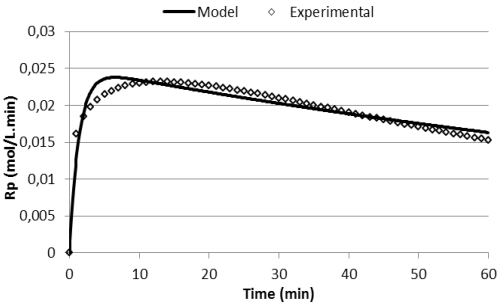

Fig. 12 Run 6

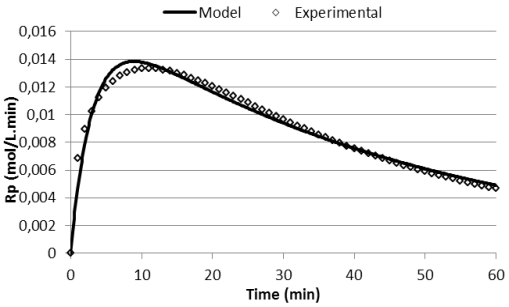

Fig. 14 Run 8

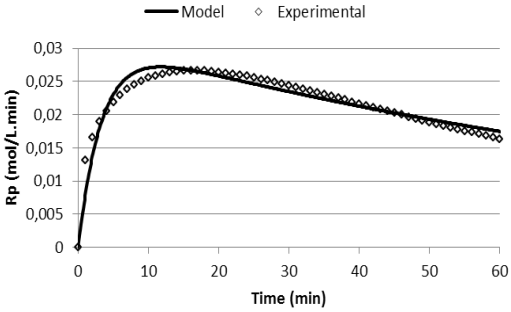

Fig. 13 Run 7

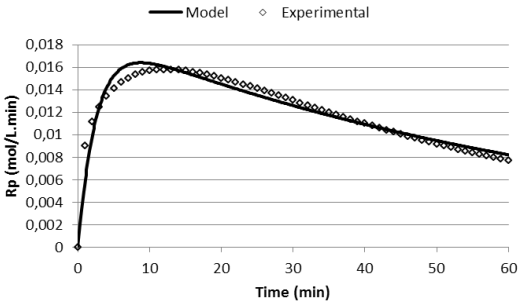

Fig. 15 Run 9

TABLE IV – KINETIC PARAMETERS FOR $(EtInd)_2ZrCl_2$ 200ºC, 450ºC AND 600ºC

Run	Catalyst type	Catalyt Mass (mg)	Pm (bar)	[C0] (mol/L)	ka (min^{-1})	kp* ($L.mol^{-1}\ bar^{-1}min^{-1}$)	kd (min^{-1})
6	$EtInd_2$ 450ºC	24	8,4	$6,27 \times 10^{-7}$	$7,16 \times 10^{-1}$	$1,56 \times 10^{4}$	$7,23 \times 10^{-3}$
7	$EnInd_2$ 450ºC	28,9	8	$5,79 \times 10^{-7}$	$3,0 \times 10^{-1}$	$1,67 \times 10^{4}$	$1,2 \times 10^{-2}$
8	$EnInd_2$ 600ºC	27,5	8,2	$1,64 \times 10^{-6}$	$3,2 \times 10^{-1}$	$8,29 \times 10^{3}$	$2,16 \times 10^{-2}$
9	$EnInd_2$ 600ºC	30	8	$2,82 \times 10^{-6}$	$3,9 \times 10^{-1}$	$8,61 \times 10^{3}$	$1,7 \times 10^{-2}$

Between the same experiments for 450ºC, we can see that there are some differences in ka and kd value. The smaller differences can be due to difficulty to get exactly the same reactor conditions in each batch, one condition was the ethylene pressure (Pm) as others.

For 600ºC the kp* is one order of magnitude less than 450ºC, meaning that the rate of monomer insertion in 600ºC case is the smallest one.

Table V, shows the kinetic parameters given by the average values of experiments obtained in the same conditions.

TABLE V – AVARAGE KINETIC PARAMETERS FOR EACH CATALYST

	n-BuCp 200ºC	n-BuCp 450ºC	n-BuCp 600ºC	EtInd2 450ºC	EtInd2 600ºC
ka	12,3	0,8395	0,344	0,509	0,34
kd	$9,06 \times 10^{-3}$	$5,26 \times 10^{-3}$	$8,15 \times 10^{-3}$	1×10^{-2}	$1,93 \times 10^{-2}$
kp	$2,24 \times 10^{4}$	$2,0 \times 10^{4}$	$1,98 \times 10^{4}$	$1,61 \times 10^{4}$	$8,49 \times 10^{3}$

5.3 Deconvolution results

$EtInd_2ZrCl_2$ 600ºC

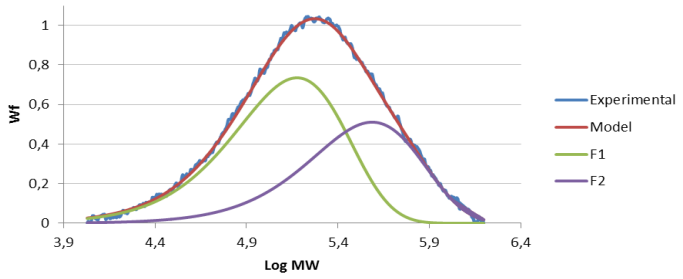

Figure 16 - MWD families of $EtInd_2$ 600ºC for 5 min

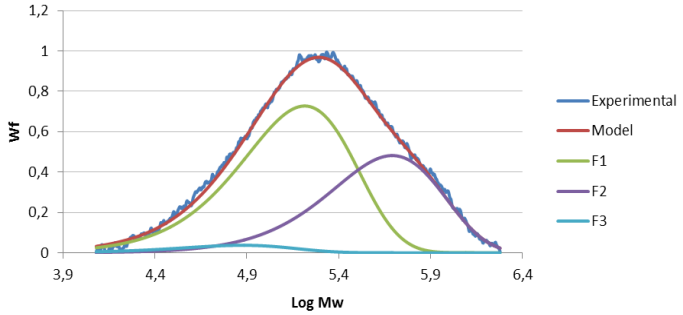

Figure 17 - MWD families of $EtInd_2$ 600ºC for 60 min

Comparing Figures 16 and 17, it is possible to notice that family one (F1) and family two (F2) maintained the same peak intensity. The main difference is the appearance of a third family after 60 minutes of reaction.

A possible interpretation for this behavior is that at the beginning of the reaction there are two types of active sites with different polymerization rates. One corresponding to the major contribution that produces the polymer chains with lower molar masses and the other that produces the higher molar masses. However after 60 minutes of reaction, a third site type appears although in a very small contribution.

From figures 18 and 19, it may be seen that between 15 and 60 minutes, the contribution of each family of active sites to the overall MWD is changing together with the average molar masses of each family. In all cases the Mn and Mw values increase from 5 to 60 minutes

So, initially the major contribution to overall MWD (m=0,58) is from the lower molar mass polymer (F2), with an average Mn around 33000, but after 60 min this lower molar mass family is centered around 45000 and its contribution decreased to only 0,13.

$EtInd_2ZrCl_2$ 450ºC

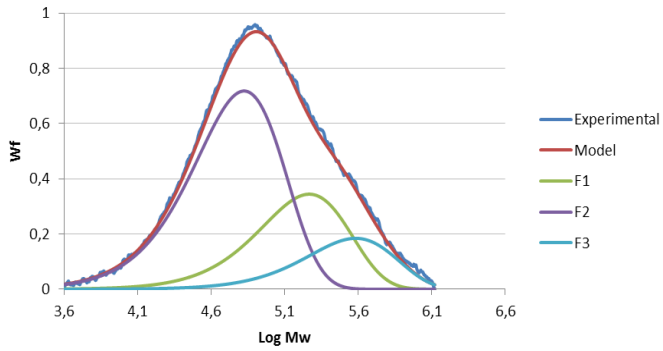

Figure 18 - MWD families of $EtInd_2$ 450ºC for 15 min

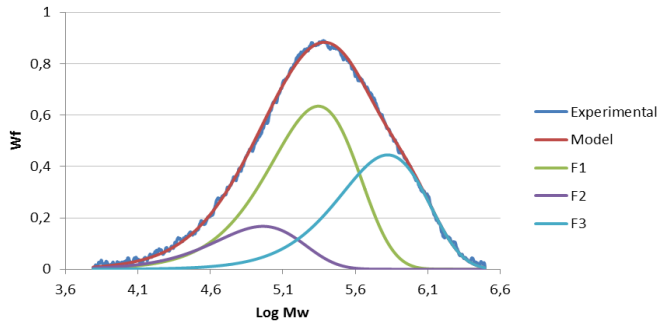

Figure 19 - MWD families of $EtInd_2$ 450ºC for 60 min

This means that the proportion of this family of active sites is decreasing along time. On the contrary the contribution of the other two families centered respectively at intermediate and higher molar masses increased considerably from 0,28 to 0,53 and from 0,15 to 0,36.

We can say also as a possible interpretation that there are 3 families, each one with different reaction behavior during the reaction. For the first family (F1), at the beginning are produced chains with considerable contribution of small molar masses. Then after 60 minutes of reaction, the same family produces chains with the same molar mass but with less contribution, meaning that propagation rate of this family is decreasing. The opposite happens with other two families, the rates of those are increasing, and after 60 minutes the second family is the one with higher molar mass impact.

Nonlinear optimization problems are frequently subject to multiple solutions, but because Flory distribution has a fixed width (PDI= 2), the MWD deconvolution procedure is generally quite robust.

I. Conclusion

Particular care had to be taken In this work, to make sure that the activity profile are representative of the experimental conditions used and reproducible. This demands using optimized and reproducible polymerization conditions from one batch to another. However the reproducibility is a difficult task to achieve in this work, due to the sensitivity of this type of catalysts to traces of water, oxygen or other polar compounds. This reflects in a difficult with experimental handling. Some of the difficulties will be mentioned below.

Some of these factors can be improved with experience time or by changing reactor configuration.

Concerning the kinetic modelling, a general model for a single site catalysts was applied and several variations of this model, with differences on the activation and deactivation steps were analyzed. Results have shown, for both type of catalyst studied, that the best fit was obtained for the non-instantaneous activation and first order deactivation model. For each system the corresponding kinetic constants ka, kp and kd, were evaluated.

The most difficult catalyst to model was n-BuCp 600ºC with X^2 values of 10^{-3} magnitude order, compared with better values of the others with $10^{-4} – 10^{-5}$ magnitude order. It was also the only experiment that wasn´t possible to get reproducibility. This may be related with the fact that temperature raises around 3ºC during one hour of reaction. For the other experiments was noticed an increase only of 0,5-1ºC.

Despite this model being mostly used for homogeneous catalyst, it revealed to be also good for this heterogeneous catalysts since the model fitted quite well the experimental data.

Regarding MWD, since these two catalysts are single site and were well fit by single site model, it was expected a PDI of 2. However for EtInd2ZrCl2 450ºC we noticed same deviation from single site once the PDI value is around 3. In fact, it was observed a good morphology for n-BuCp with a spherical powder not sticky and on the other hand for EtInd2 the polymer was a very sticky powder.

This could be related with use of TiBA. TiBA act as a scavenger cleaning all the impurities remain in solvent, argon and ethylene compounds. The volume of TiBA added is the optimized volume for not affecting reaction rate (getting from some previous studies). However TiBA could also somehow interferes with reaction affecting not only activity but also the polymer microstructure. To confirm that TiBA affects the microstructure was performed an experiment with TEA and was obtain similar powder to n-BuCp althought with less activity. Meaning that TEA could be a better choice than TiBA in future experiments.

Although we could get some conclusion from results, there are some factors that need to be considered. The way the polymer sample is dried is very important, because remains of any solvent are evaporated and interferes with crystallinity and melting point measures. Also the remains of catalyst, although are in less quantity than polymer, could have some interference. Considering these factors and also a DSC accuracy of ±5% on the crystallinity measurement, it is necessary to repeat again the same experiments to conclude precise results.

References

[1] CHAKRAVARTI, S.; RAY, W. Harmon (2001) Kinetic study of olefin polymerization with a supported metallocene catalyst. Ethylene/1-hexene copoymerization in gas phase, Wisconsin, Journal of Applied Polymer Science 80, 1096-1119

[2] MCKENNA, T.F.L; SOARES, J.B.P; (2012) Polyolefin Reaction Engineering, Germany: Wiley-VCH

[3] MCKENNA, Timothy F.; SOARES, João B.P (2001) Single particle modelling for olefin polymerization on supported catalyst: A review and proposals for future developments, Canada, Chemical Engineering Science 56, 3931-3949

[4] TISSE, Virginie F.; BOISSON, Christophe; MCKENNA, Timothy F.L. (2014) Activation and deactivation of the polymerization of ethylene over rac-EtInd2ZrCl2 and (n-BuCp)2ZrCl2 on na activating silica support, Macromol. Chem. Phys, DOI, 10.1002

[5] CHIN-SAN, (2008) Handbook Of Size Exclusion Chromatography And Related Technique, p. 488

[6] Hasan A.T.M. Kamrul, Multiplicity of active-sites in heterogeneous Ziegler-Natta catalyst and it´s correlation with polymer microstructure, Bangladesh J.Sci Ind. Res. 46 (6), 487-494, 2011

[7] HAN, Joong Jin; LEE, Hyung Woo; YOON, Won Jung; CHOI, Kyu Yong, (2007), Rate and molecular weight distribution modeling of syndiospecific styrene polymerization over silica-supported metallocene catalyst, Korea, Elsevier Ltd, Polymer 48, 6519-6531

[8] BERGSTRA, Michiel F.; WEICKERT, Gunter (2006) Semi-batch reactor for kinetic measurements of catalyzed olefin co-polymerizations in gas and slurry phase, Chemical Engineering Science 61, 4909-4918

[9] GRIEKENM, R. Van; CARRERO, A.; PAREDES, B.; SUAREZ, I. (2007) Ethylene polymerization over supported MAO/ (n-BuCp)2ZrCl2 catayst: Influence of support properties, Spain, European Polymer Journal 43, 1267-1277

[10] BOCHMANN, Manfred (2004) Kinetic and mechanistic aspects of metallocene polymerization catalyst, UK, Journal of Organometallic Chemistry 689 3982-3998

[11] TIONI, Estevan; BROYER, Jean Pierre; MONTEIL, Vincent; MCKENNA, Timothy (2012) Influence of reaction conditions on catalyst behavior during the early stages of gas phase ethylene homo- and copolymerization, Netherlands, Ind. Eng. Chem. 51, 14673-14684

[12] MCAULEY, Kim B.; HSU, James C.C.; BACON, David W. (2005) Mathematical model and parameter estimation for gas-phase ethylene/hexene copolymerization with metallocene catalyst, Canada, Macromol. Mater. Eng 290, 537-557

[13] MOGILICHARLA, Anitha; MITRA Kishalay; MAJUMDAR, Saptarshi (2014) Modeling of propylene polymerization with long chain branching, India, Chemical Engineering Journal 246, 175-183

[14] MCAULEY, Kim B.; KOU, Bo (2005) Mathematical model and parameter estimation for gas-phase ethylene homopolymerization with supported metallocene catalyst, Canada, Ind.Eng. Chem. Res. 44 2428-2442